ACS OMEGA

Article

Cite This: ACS Omega 2018, 3, 9710−9721

http://pubs.acs.org/journal/acsodf

Synthesis and Postpolymerization Modification of Fluorine-End-Labeled Poly(Pentafluorophenyl Methacrylate) Obtained via RAFT Polymerization

Claudia Battistella,[†] Yuejiao Yang,[‡] Jie Chen,[‡] and Harm-Anton Klok*[,†]

[†]Institut des Matériaux et Institut des Sciences et Ingénierie Chimiques, Laboratoire des Polymères, École Polytechnique Fédérale de Lausanne (EPFL), Bâtiment MXD, Station 12, CH-1015 Lausanne, Switzerland

[‡]School of Environmental and Chemical Engineering, Shanghai University, 200444 Shanghai, China

Supporting Information

ABSTRACT: Chain-end-labeled polymers are interesting for a range of applications. In polymer nanomedicine, chain-end-labeled polymers are useful to study and help understand cellular internalization and intracellular trafficking processes. The recent advent of fluorescent label-free techniques, such as nanoscale secondary ion mass spectrometry (NanoSIMS), provides access to high-resolution intracellular mapping that can complement information obtained using fluorescent-labeled materials and confocal microscopy and flow cytometry. Using poly(*N*-(2-hydroxypropyl)methacrylamide) (PHPMA) as a prototypical polymer nanomedicine, this paper presents a synthetic strategy to polymers that contain trace element labels, such as fluorine, which can be used for NanoSIMS analysis. The strategy presented in this paper is based on reversible addition fragmentation chain transfer (RAFT) polymerization of pentafluorophenyl methacrylate (PFMA) mediated by two novel chain-transfer agents (CTAs), which contain either one (α) or two (α,ω) fluorine labels. In the first part of this study, via a number of polymerization experiments, the polymerization properties of the fluorinated RAFT CTAs were established. ^{19}F NMR spectroscopy revealed that these fluorinated RAFT agents possess unique spectral signatures, which allow to directly monitor RAFT agent conversion and measure end-group fidelity. Comparison with 4-cyanopentanoic acid dithiobenzoate, which is a standard CTA for the RAFT polymerization of PFMA, revealed that the introduction of one or two fluorine labels does not significantly affect the polymerization properties of the CTA. In the last part of this paper, a proof-of-concept study is presented that demonstrates the feasibility of the fluorine-labeled poly(pentafluorophenyl methacrylate) polymers as platforms for the postpolymerization modification to generate PHPMA-based polymer nanomedicines.

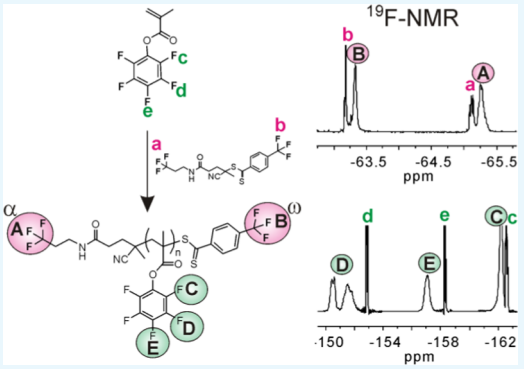

INTRODUCTION

Polymers containing labels, such as fluorescent dyes, are of interest for a myriad of applications. One example of the use of fluorescent-labeled polymers is in polymer nanomedicine. Fluorescent-labeled polymers are extensively used to monitor internalization and intracellular trafficking of polymers and polymer nanoparticles. A number of strategies have been developed for the synthesis of fluorescent-labeled polymers, which lead to incorporation of the dye label either as a side-chain functionality or at the chain end.[1] Chain-end labeling is very attractive since only a very small number of dye labels are required and the polymer side chains are frequently used to anchor bioactive cargo.[1]

Controlled radical polymerization techniques are very powerful tools for the preparation of chain-end-labeled polymers as they preserve reactive polymer chain ends throughout the polymerization reaction.[1] Reversible addition fragmentation chain transfer (RAFT) polymerization, in particular, is a very attractive method for the preparation of chain-end-labeled polymers that are to be used as polymer nanomedicines or for other biological applications.[2] The RAFT polymerization method is characterized by an exceptional functional group tolerance.[2,3] By adjusting the nature of the R and Z groups of the chain-transfer agent (CTA), RAFT polymerization can be used to generate polymers that contain functional groups at the α- and ω-chain ends.[2−6] Fluorescent chain-end-labeled polymers have been prepared by RAFT polymerization by reduction of the CTA-derived end group, followed by reaction with a maleimide-modified fluorescent dye.[7] Alternatively, the thiol end groups on polymers obtained by RAFT polymerization have been reacted with cystamine, followed by coupling of an NHS ester fluorescent dye.[8]

Although they have been extensively used to monitor and study cellular uptake and intracellular trafficking of polymers

Received: July 13, 2018
Accepted: August 9, 2018
Published: August 22, 2018

Chart 1. Chemical Structures of 4-Cyanopentanoic Acid Dithiobenzoate (CTA-1), R-Labeled CTA (F-CTA-1), and R−Z-Labeled CTA (F-CTA-2)

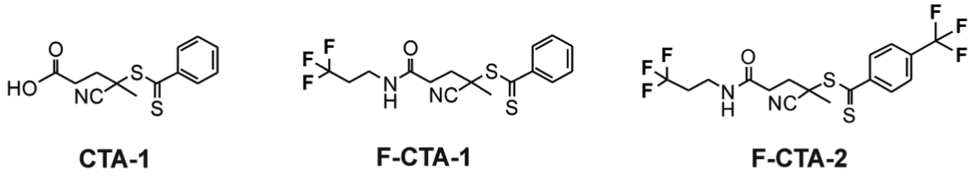

Scheme 1. Synthesis of Fluorinated End-Labeled PPFMA Using F-CTA-1 and F-CTA-2

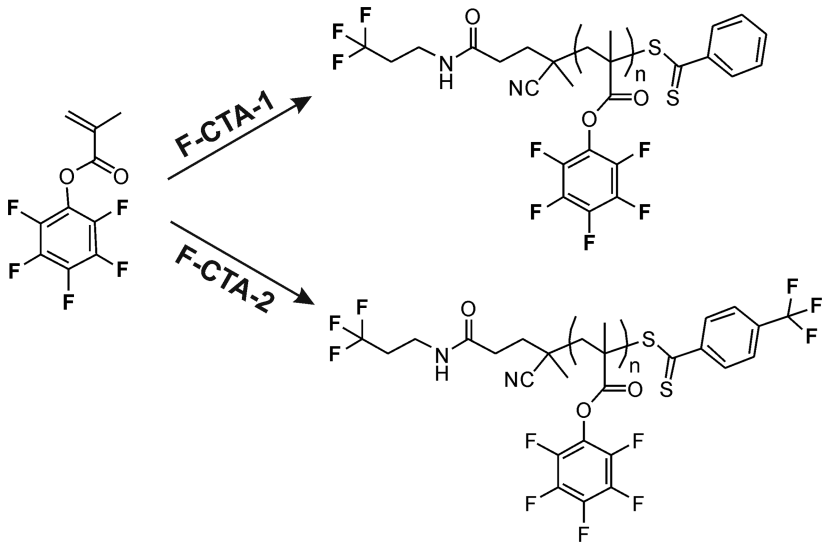

and polymer nanoparticles, fluorescent dyes also have some drawbacks and limitations. Exposure of polymer−dye conjugates or dye-loaded nanoparticles to the highly degradative intracellular environment can result in release of the dye.[9,10] Another potential limitation is the risk for pH- and concentration-dependent quenching or photobleaching.[9−12] Finally, the fluorescent dye may alter the uptake or internalization properties of the polymer[13] and/or influence intracellular processes.[14]

Over the past years, the number of techniques available to study cell uptake and intracellular trafficking of polymers and polymer nanoparticles has increased and now also includes several methods that do not require the use of fluorescently labeled polymers.[15] Raman spectroscopy, for example, uses vibrational labels, often isotopes,[16−19] and nanoscale secondary ion mass spectrometry (NanoSIMS) allows the intracellular tracking of trace elements or isotopes.[20−22] Synchrotron X-ray fluorescence imaging has also been used to visualize elements and metals in cellular environments.[23−25] As a consequence, there is an increasing demand for simple and efficient methods to label polymers with isotopes and trace elements. Among the various trace elements or isotopes that are available, fluorine is very attractive as it gives rise to minimal steric alterations and possesses a high metabolic stability.[26] A number of techniques have been developed, which take advantage of these favorable attributes of fluorine, such as Fluoro-Raman spectroscopy[27,28] and ^{19}F-magnetic resonance imaging (^{19}F-MRI). In the literature, a number of side-chain-fluorinated polymers have been reported, which were used for ^{19}F-MRI studies.[29,30]

One possible strategy for the preparation of fluorine-end-labeled polymers is via RAFT polymerization using fluorinated CTAs. There are a number of reports in the literature that describe the use of fluorinated RAFT agents. Fluorinated RAFT agents have been used in the polymerization of a variety of monomers, including ethyl acrylate, styrene, methyl methacrylate, butyl acrylate, vinyl pyrrolidone, vinyl chloride, and vinyl acetate. In most instances, the introduction of fluorine was explored to modulate the reactivity of the RAFT agent.[31−37] In other examples, fluoralkyl-functionalized RAFT agents were used to prepare polymers and copolymers with perfluorinated end groups.[38,39] These chain-end-fluorinated polymers were used as additives to modify the surface properties of the corresponding nonfluorinated polymers.[39]

So far, the use of fluorinated RAFT CTAs for the polymerization of active ester monomers has not been explored. This approach, however, would offer a number of opportunities for the preparation of polymer nanomedicines. First, since the fluorine labels are only introduced at the chain end(s) of the resulting polymers, any impact on the solution properties of the polymers is expected to be negligible/reduced compared to the use of side-chain-fluorinated polymers. Second, while the fluorine-chain-end-functional groups can be exploited as labels for bioimaging purposes, the active ester side chains can be utilized for further postpolymerization modification reactions to introduce, for example, bioactive cargo. Finally, due to its unique sensitivity, fluorine labeling of the RAFT agent may also allow to directly monitor RAFT agent conversion and end-group fidelity of the produced polymers by ^{19}F NMR spectroscopy.

In this paper, we describe the preparation of fluorine-chain-end-labeled side-chain-reactive polymers via RAFT polymerization of pentafluorophenyl methacrylate (PFMA). PFMA is a side-chain-reactive monomer, which can be polymerized via RAFT polymerization and which is widely used for the

DOI: 10.1021/acsomega.8b01654
ACS Omega 2018, 3, 9710−9721

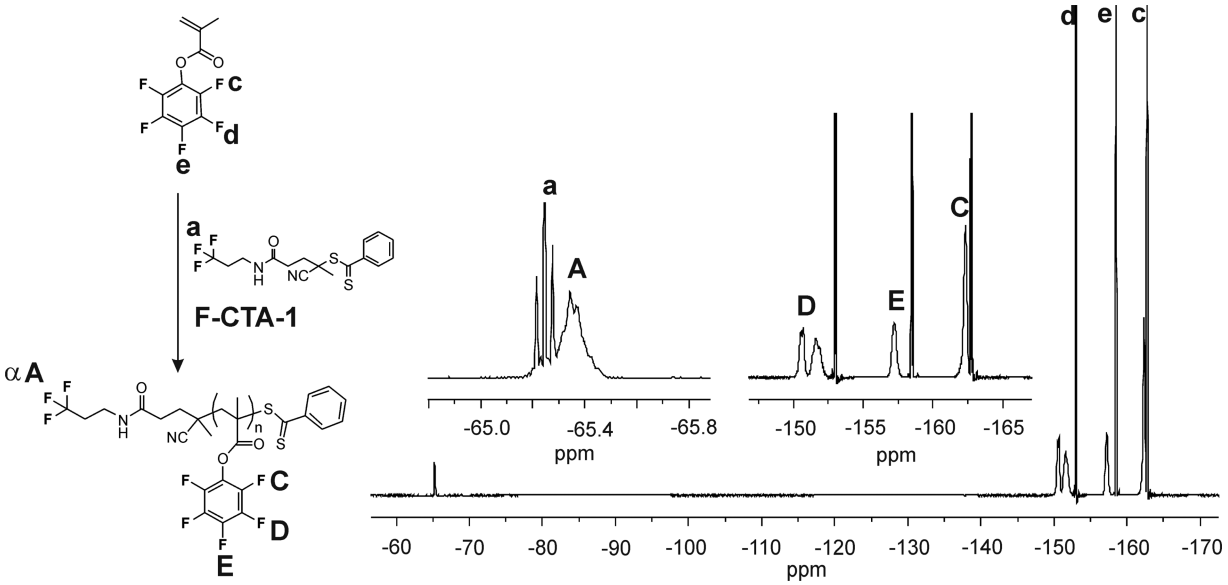

Figure 1. Example of a ^{19}F NMR spectrum of α-fluorinated PPFMA obtained using **F-CTA-1**. Polymerization conditions: dioxane; 75 °C; $[M]_0$ = 1.8 M; $[M]_0$:$[\textbf{F-CTA-1}]_0$ = 100, $[\textbf{F-CTA-1}]_0$:$[I]_0$ = 10; polymerization time, 300 min. The inset is a magnification of a selected area of the spectrum to highlight the polymer-derived ^{19}F NMR signals (A–E).

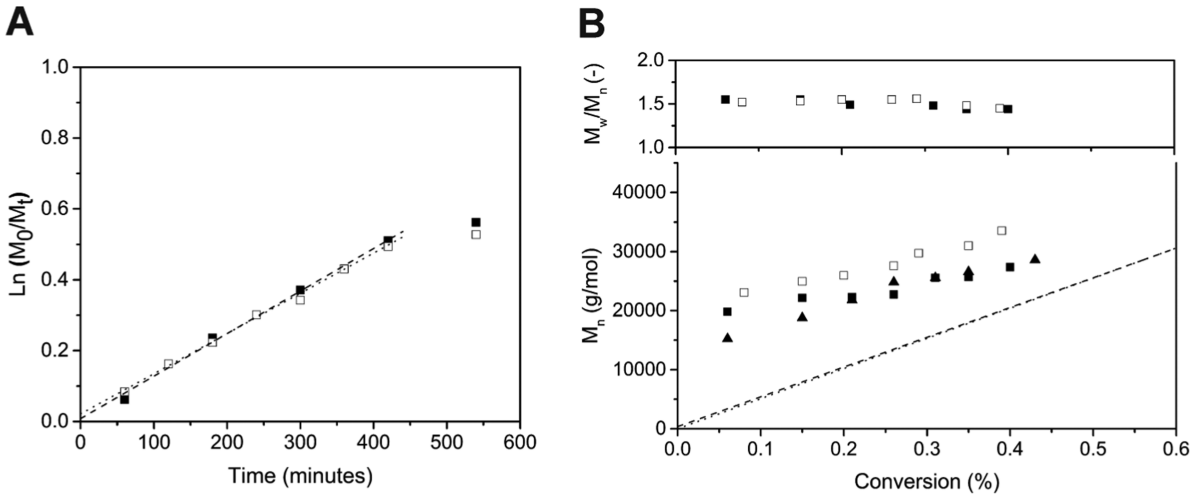

Figure 2. (A) First-order kinetic plot for the RAFT polymerization of PFMA as determined by ^{19}F NMR spectroscopy. Polymerization conditions: dioxane; 75 °C; $[M]_0$ = 1.8 M; $[CTA]_0$:$[I]_0$ = 10; $[M]_0$:$[\textbf{CTA-1}]_0$ = 200 (□); and $[M]_0$:$[\textbf{F-CTA-1}]_0$ = 200 (■). (B) Evolution of experimental M_n and M_w/M_n as a function of monomer conversion for **CTA-1** as determined by SEC (□) and **F-CTA-1** as determined by SEC (■) and ^{19}F NMR (▲). SEC analysis was performed using THF as solvent and PS standards were used for conventional calibration. The dotted lines (**CTA-1**) and dashed lines (**F-CTA-1**) indicate the expected theoretical M_n (M_n^{TH}).

preparation of reactive polymer precursors.[40,41] For the RAFT polymerization, two different fluorinated chain-transfer agents (CTAs) were used, which contain either one (R) or two (R,Z) fluorine labels. After investigating the feasibility of the two fluorinated RAFT agents to mediate the polymerization of PFMA, the postpolymerization modification of the resulting poly(pentafluorophenyl methacrylate) (PPFMA) polymers to generate α-fluorine, ω-Rhodamine Red end-labeled poly(*N*-(2-hydroxypropyl)methacrylamide) (PHPMA) will be reported. PHPMA is interesting as a proof of concept since this polymer has been widely used for the preparation of polymer–drug conjugates.[42−53]

RESULTS AND DISCUSSION

Design and Synthesis of the Fluorinated CTAs. Eberhardt et al. investigated the RAFT polymerization of PFMA using cumyl dithiobenzoate and 4-cyanopentanoic acid dithiobenzoate as chain-transfer agents.[51] Both CTAs have an activating phenyl Z group and a good tertiary cumyl or cyanopentanoic acid leaving radical R$^\bullet$, which are suitable for activated monomers, such as methacrylates. These studies revealed that 4-cyanopentanoic acid dithiobenzoate was a more effective chain-transfer agent for the RAFT polymerization of PFMA compared to cumyl dithiobenzoate.[51] 4-Cyanopentanoic acid dithiobenzoate (here after referred to as **CTA-1**) since then has been extensively used for the RAFT polymerization of PFMA[43,44,46,47] and also served as the precursor and starting point for the design of the fluorinated CTAs

DOI: 10.1021/acsomega.8b01654
ACS Omega 2018, 3, 9710−9721

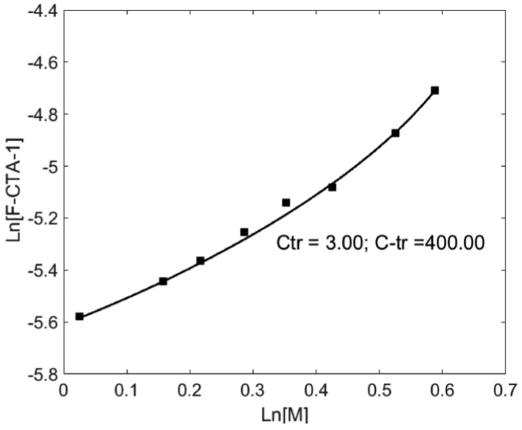

Figure 3. Double-logarithmic plot of [**F-CTA-1**] vs [M] as determined by ^{19}F NMR spectroscopy. The experimental points were fitted using eq 4. Polymerization conditions: dioxane; 75 °C; $[M]_0$ = 1.8 M; $[M]_0$:[**F-CTA-1**]$_0$ = 200; [**F-CTA-1**]$_0$:$[I]_0$ = 10.

investigated in this study. The chemical structures of **CTA-1** and the two fluorinated derivatives investigated in this study are shown in Chart 1. While **F-CTA-1** contains a trifluoromethyl label in the R group, **F-CTA-2** contains two trifluoromethyl labels in both the R and the Z groups. The synthesis of **F-CTA-1** and **F-CTA-2** is presented in Scheme S1. A number of factors were taken into account for the selection of fluorinated labels as well as their position in the CTA. First of all, to be able to characterize the polymer end groups and to monitor the progress of the polymerization by ^{19}F NMR spectroscopy, two different labels are needed with ^{19}F NMR chemical shifts that overlap neither with each other nor with those of the PFMA units of the monomer or polymer. A second prerequisite is that the introduction of the labels should not affect the polymerization process (vide infra). **F-CTA-1** was obtained in a single step via *N*-(3-dimethylaminopropyl)-*N*′-ethylcarbodiimide (EDC)-mediated coupling of **CTA-1** with 3,3,3-trifluoropropylamine hydrochloride. Compared to **F-CTA-1**, **F-CTA-2** contains a trifluoromethylphenyl Z-group as a second fluorine label. Previous work has shown that the introduction of electron-withdrawing groups (such as trifluoromethyl) on the phenyl Z-group of dithioester CTAs increases the activity of the RAFT agent and resulted in narrow molecular-weight distributions at low conversion.[34] The remainder of this paper will first discuss the RAFT polymerization of PFMA with **F-CTA-1** and investigate the effect of various reaction parameters, such as temperature and the $[M]_0$:$[CTA]_0$ ratio (Scheme 1). After that, the optimal RAFT polymerization conditions that have been identified using **F-CTA-1** will be used in the **F-CTA-2**-mediated RAFT polymerization of PFMA.

F-CTA-1-Mediated Polymerization of PFMA. RAFT polymerization of PFMA mediated by **CTA-1** is generally performed in dioxane using monomer concentrations ($[M]_0$) of 2 M, $[CTA]_0$:$[I]_0$ ratios of 8−10[44,47,51,52] as well as relatively low reaction temperatures (65−75 °C)[47,52,53] and long polymerization times (up to 42 h).[47] To the best of our knowledge, however, a detailed study of the polymerization kinetics of PFMA under these conditions has not been reported. Eberhardt et al. reported the kinetics of the RAFT polymerization of PFMA using **CTA-1** at a monomer concentration of ∼2 M and a 8:1 $[CTA]_0$:$[I]_0$ ratio. These polymerizations were carried out at 90 °C, and the highest obtained molecular weight (M_n) was around 10 000 g/mol.[51] In the present study, first a set of experiments was performed to investigate and compare the kinetics of the RAFT polymerization of PFMA with **CTA-1** and **F-CTA-1**. These polymerizations were carried out in dioxane at 75 °C using 2,2′-azobis(2-methylpropionitrile) (AIBN) as the initiator at $[M]_0$ = 1.8 M, $[CTA]_0$:$[I]_0$ = 10, and $[M]_0$:$[CTA]_0$ = 200. Polymerization reactions were monitored by ^{19}F NMR spectroscopy. An example of a ^{19}F NMR spectrum of an aliquot taken from a polymerization reaction is shown in Figure 1. The spectrum illustrates the unique sensitivity of ^{19}F. Due to the difference in chemical shift of the free and polymerized PFMA as well as that between the free and polymer-bound **F-CTA-1** agent, not only the monomer conversion but also the consumption of the RAFT agent, can be directly determined from the ^{19}F NMR spectra. Furthermore, comparison of the integrals of the fluorinated polymer end groups to that of the PPFMA side chains provides the degree of polymerization. Monomer conversion ρ (%) was determined by ^{19}F NMR spectroscopy, taking advantage of the difference in ^{19}F NMR chemical shifts of the pentafluorophenyl ester groups in the monomer (c, d, e) and polymer (C, D, E) as shown in Figure 1. The monomer conversion at a given polymerization time was determined using eq 1 by comparing the area of the polymer peaks to that of the remaining monomer peaks indicated in Figure 1 as **E** and **e**, respectively.

$$\rho\ (\%) = \frac{\int \mathbf{E}}{\int \mathbf{E} + \int \mathbf{e}} \times 100 \qquad (1)$$

Subsequently, the monomer conversion ρ, the initial $[M]_0$:$[CTA]_0$ ratio, and the number of initiator (AIBN)-derived side chains ($df([I]_0 - [I])$) were used to calculate the theoretical degree of polymerization, as shown in eq 2.[54] $df([I]_0 - [I])$ was expressed as $df[I]_0(1 - e^{-k_d t})$, where k_d is the rate constant for initiator decomposition at 75 °C (7.33×10^{-5} s^{-1}) and 90

Table 1. C_{tr} and C_{-tr} Values for the Different PFMA Polymerization Conditions Using F-CTA-1 and F-CTA-2

F-CTA	$[M]_0$ (mol/L)	$[M]_0$:$[F\text{-}CTA]_0$	$[F\text{-}CTA]_0$:$[I]_0$	temperature (°C)	C_{tr}[a]	C_{-tr}[a]
F-CTA-1	1.8	200	10	75	3.0	400.0
		100	10	75	3.2	390.0
				90	4.1	399.9
		50	10	75	3.5	390.0
				90	4.7	391.0
F-CTA-2		100	10	90	4.0	390.1
		50	10	90	4.8	370.1

[a]Determined using eq 4.

DOI: 10.1021/acsomega.8b01654
ACS Omega 2018, 3, 9710−9721

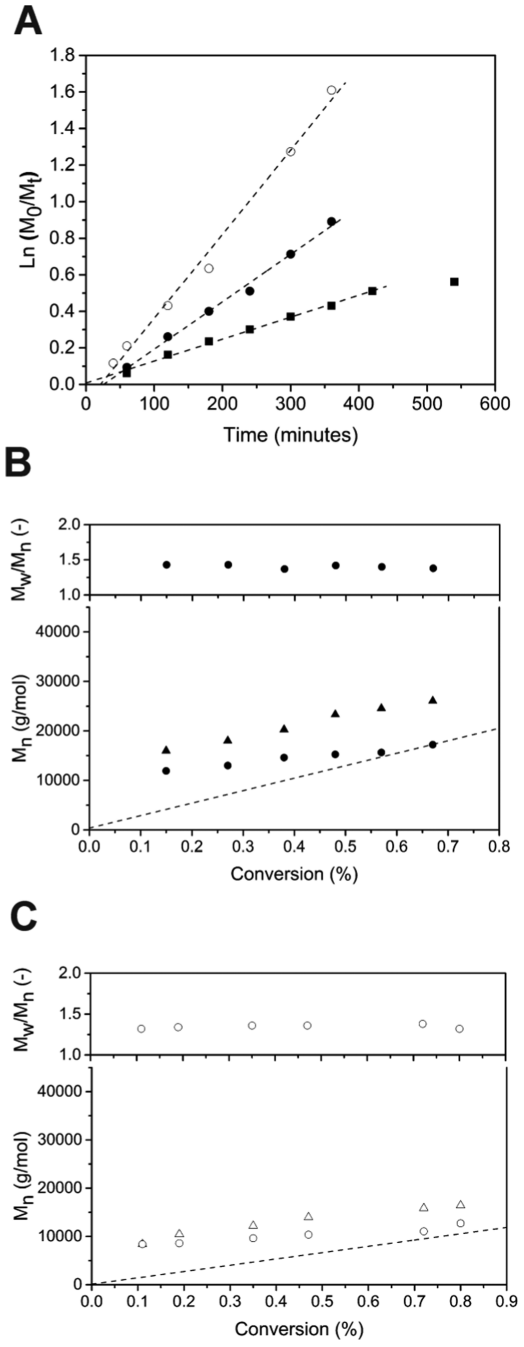

Figure 4. (A) First-order kinetic plots for the RAFT polymerization of PFMA as determined by ^{19}F NMR spectroscopy. Polymerization conditions: dioxane; 75 °C; $[M]_0$ = 1.8 M; $[M]_0$:[**F-CTA-1**]$_0$ = 200 (■), 100 (●), and 50 (○); and [**F-CTA-1**]$_0$:$[I]_0$ = 10. (B) Evolution of experimental M_n and M_w/M_n as a function of monomer conversion for $[M]_0$:[**F-CTA-1**]$_0$ = 100 as determined by SEC (●) and ^{19}F NMR (▲) and (C) $[M]_0$:[**F-CTA-1**]$_0$ = 50 as determined by SEC (○) and ^{19}F NMR (Δ). SEC analysis was performed using THF as solvent and PS standards were used for conventional calibration. The dashed lines indicates the theoretical M_n (M_n^{TH}) expected for the different conditions.

°C (4.79×10^{-4} s^{-1}),[55] f is the initiator efficiency, which is assumed to be 0.6 (f = 0.6),[55−57] and d is the number of chains produced in a radical−radical termination event. Since this value is not available for this specific system, the value reported for MMA was used (d = 1.67).[56,57] The theoretical molecular weights (M_n^{TH}) were calculated taking into account the monomer (mM) and the CTA (mCTA) molecular weights as given in eq 3. Experimental molecular weights of the polymers obtained using both **CTA-1** and **F-CTA-1** for the different polymerization times were determined by size exclusion chromatography (SEC) analysis using tetrahydrofuran (THF) as solvent and polystyrene (PS) as standard. While this eluent and standard have been previously used for the SEC analysis of PPFMA,[45] the hydrodynamic properties of PPFMA and PS in THF may not be comparable. As illustrated by Figure 1, however, ^{19}F NMR spectroscopy can be used to validate the SEC molecular weights. ^{19}F NMR number-average molecular weights (M_n) were determined by comparing the integrals of the ^{19}F NMR signal generated by the three fluorine atoms at the α-end group of PPFMA (A in Figure 1) to that of the PFMA polymer side chains (E).

$$DP^{TH} = \rho \frac{[M]_0}{[CTA]_0 + df[I]_0(1 - e^{-k_d t})} \quad (2)$$

$$M_n^{TH} = DP^{TH} \times mM + mCTA \quad (3)$$

Figure 2 and Table S1 summarize the results of the analysis of RAFT polymerization experiments of PFMA with **CTA-1** and **F-CTA-1**, which were carried out in dioxane at 75 °C, $[M]_0$ = 1.8 M, $[CTA]_0$:$[I]_0$ = 10, and $[M]_0$:$[CTA]_0$ = 200. For both the **CTA-1**- and **F-CTA-1**-mediated RAFT polymerization of PFMA, first-order kinetic plots were obtained (Figure 2A) and in both cases, the experimental polymer molecular weights were found to increase linearly with monomer conversion. Also the polydispersities of polymers produced with the two different RAFT agents were comparable and slightly decreased with increasing monomer conversion (Figure 2B). The relatively good agreement between the results obtained using **CTA-1** and **F-CTA-1** suggests that the modification of **CTA-1** with a fluorine label does not seem to influence the reactivity of the RAFT agent toward the polymerization of PFMA. For both the **CTA-1**- and **F-CTA-1**-mediated RAFT polymerization, especially in the early stages of the polymerization, however, it was observed that the experimental molecular weights were higher than the theoretical predictions. This, together with relatively high polydispersity values (>1.5) in the early stages of the polymerization process, indicates a slow consumption of the CTAs. The relatively slow consumption of the CTAs is also evident from the ^{19}F NMR spectra shown in Figure 1. In this spectrum, the ^{19}F signal due to the CF_3 group of the nonreacted **F-CTA-1** can be clearly observed next to that of the **F-CTA-1**, which has been incorporated in the polymer. In an ideal case, the degree of polymerization at a particular polymerization time is expressed as $([M]_0 - [M])$:$[CTA]_0$. Therefore, a CTA that is slowly consumed generates polymer chains having an experimental molecular weight higher than expected. The early stage of the **CTA-1**- and **F-CTA-1**-mediated polymerization of PFMA therefore proceeds via a hybrid free-radical RAFT mechanism.[34,57,58] As the polymerization time increases, the higher CTA conversion shifts the process toward a RAFT mechanism and the experimental molecular weights converge toward the theoretical values.

Determination of the Transfer Constants C_{tr} and C_{-tr} of F-CTA-1. To assess the efficiency of **F-CTA-1**, the transfer constants C_{tr} ($=k_{tr}/k_p$) and C_{-tr} ($=k_{-tr}/k_{iR}$), which take into account the reactivity of the propagating radical $P_n^{\bullet}$ and the

DOI: 10.1021/acsomega.8b01654
ACS Omega 2018, 3, 9710−9721

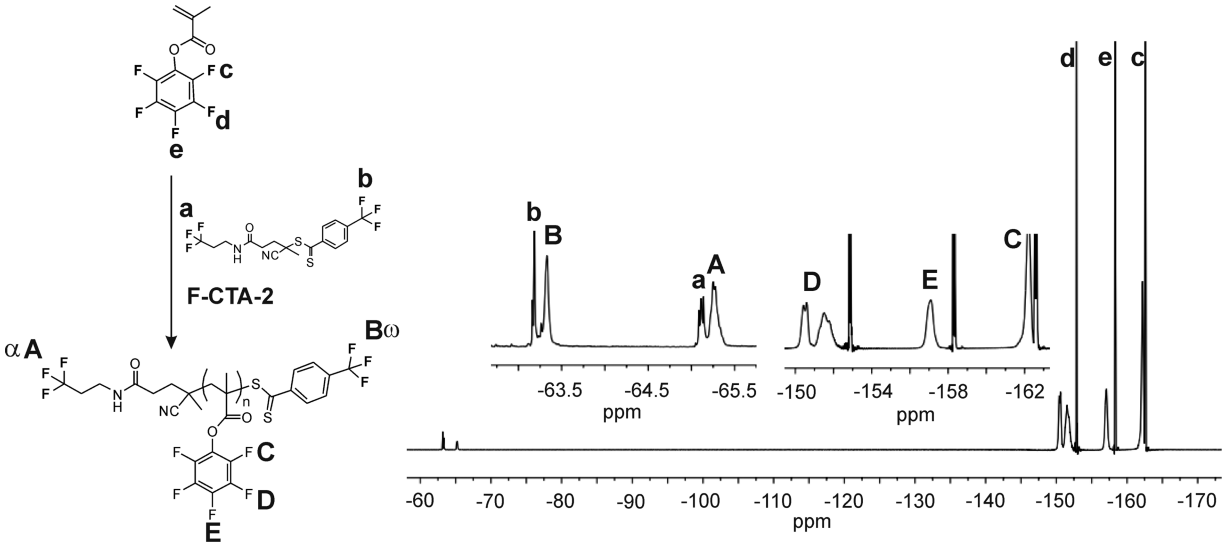

Figure 5. Example of an ^{19}F NMR spectrum of α,ω-fluorinated PPFMA obtained using **F-CTA-2**. Polymerization conditions: dioxane, 90 °C, $[M]_0$ = 1.8 M, $[M]_0$:[**F-CTA-2**]$_0$ = 100, [**F-CTA-2**]$_0$:$[I]_0$ = 10, polymerization time 240 min.

reactivity of the expelled radical R$^\bullet$, were determined from the decay of the CTA concentration during the polymerization using the following equation[54,56,58]

$$\frac{d[CTA]}{d[M]} \approx C_{tr}\frac{[CTA]}{[M] + C_{tr}[CTA] + C_{-tr}[\mathbf{2}]} \quad (4)$$

where [CTA] and [M] are the CTA and monomer concentrations at a particular polymerization time, respectively, and [**2**] is the concentration of dormant polymer chains, which can be directly related to the [CTA] and the initial CTA concentration $[CTA]_0$. Hence, if both monomer and CTA consumptions can be experimentally determined at each polymerization time, eq 4 can be fitted using independent pairs of input C_{tr} and C_{-tr}.[56,57,59] Usually, CTA conversion is estimated by comparing the found and theoretically expected number-average molecular weights.[56] For some RAFT agents, CTA conversion has been directly monitored by ^{1}H NMR spectroscopy, but for others, overlap with resonances due to the polymer often prevents the use of ^{1}H NMR analysis.[60] As shown in Figure 1, ^{19}F NMR spectroscopy is a powerful method to directly monitor CTA conversion. The ^{19}F label in **F-CTA-1** allows to distinguish between free (the signal labeled as "a" in Figure 1) and bound CTA (the signal labeled as "A" in Figure 1) and thus to directly determine **F-CTA-1** consumption by ^{19}F NMR analysis. As an example, Supporting Information Figures S1−S4 show ^{19}F NMR spectra of samples taken from the **F-CTA-1**-mediated polymerization of PFMA at $[M]_0$:$[CTA]_0$ = 50 at 20, 40, 60, and 120 min polymerization time, which illustrate the consumption of the CTA with increasing reaction time. Figure 3 plots the evolution of **F-CTA-1** conversion with increasing monomer conversion in a double-logarithmic fashion for a RAFT polymerization of PFMA with **F-CTA-1** at $[M]_0$:$[CTA]_0$ = 200 and $[CTA]_0$:$[I]_0$ = 10 at a polymerization temperature of 75 °C. Fitting of the experimental data with eq 4 allowed the determination of C_{tr} and C_{-tr}, which were found to be 3 and 400, respectively. For a RAFT polymerization to display the typical characteristics of a "living"/controlled polymerization reaction, a C_{tr} of at least 10 is required.[58] Very effective RAFT agents usually have C_{tr} > 100. In an attempt to improve control of the polymerization, a number of further experiments, in which the $[M]_0$:[**F-CTA-1**]$_0$ ratio (from 200 to 100 and 50) as well as the polymerization temperature (90 °C instead of 75 °C) was varied, were performed and C_{tr} and C_{-tr} were determined using the same procedure. Table 1 lists the C_{tr} and C_{-tr} values determined from these experiments. The corresponding plots of ln[**F-CTA-1**] versus ln[M] and the respective fits are included in Supporting Information Figure S5. The results in Table 1 suggest a minor increase in C_{tr} upon increasing the polymerization temperature as well as upon decreasing $[M]_0$:$[CTA]_0$ at a given temperature. Analysis of the corresponding polymerization kinetics, as well as of the evolution of polymer molecular weight and polydispersity upon decreasing $[M]_0$:$[CTA]_0$ or increasing the polymerization temperature to 90 °C, however, still points toward a hybrid-type polymerization behavior and no significant improvement in M_w/M_n was observed (see Figure 4 for T = 75 °C and Supporting Information Figure S6 for T = 90 °C).

RAFT Polymerization of PFMA Using F-CTA-2. **F-CTA-2** contains a fluorinated label in both the R(α) and Z(ω) groups. As illustrated in Figure 5, the fluorinated chain ends derived from the R and Z groups of **F-CTA-2** give rise to different ^{19}F NMR chemical shifts. This is attractive as it does not only allow to use ^{19}F NMR spectroscopy to directly monitor **F-CTA-2** consumption during polymerization, but also to assess end-group fidelity by comparison of the integrals associated to the α (A) and ω (B) chain-end-terminal CF_3 groups. Polymerization experiments with **F-CTA-2** were carried out at 90 °C using both $[M]_0$:$[CTA]_0$ = 100 and $[M]_0$:$[CTA]_0$ = 50. Table S2 summarizes the results of these experiments, and Figure 6 shows the polymerization kinetics as well as evolution of polymer molecular weight for these polymerization experiments. The polymerization kinetics using **F-CTA-2** were slightly slower compared to the **F-CTA-1**-mediated polymerization of PFMA (see Supporting Information Figure S6). Similar to what was observed for **F-CTA-1**, the experimental molecular weights, in particular at low monomer conversion, were higher than the expected polymer molecular weights. To explain these observations, C_{tr} and C_{-tr} were determined as discussed above for **F-CTA-1**. Examples of ^{19}F NMR spectra of the polymers obtained using $[M]_0$:$[CTA]_0$ = 50 are reported in Supporting Information Figures S7−S10.

DOI: 10.1021/acsomega.8b01654
ACS Omega 2018, 3, 9710−9721

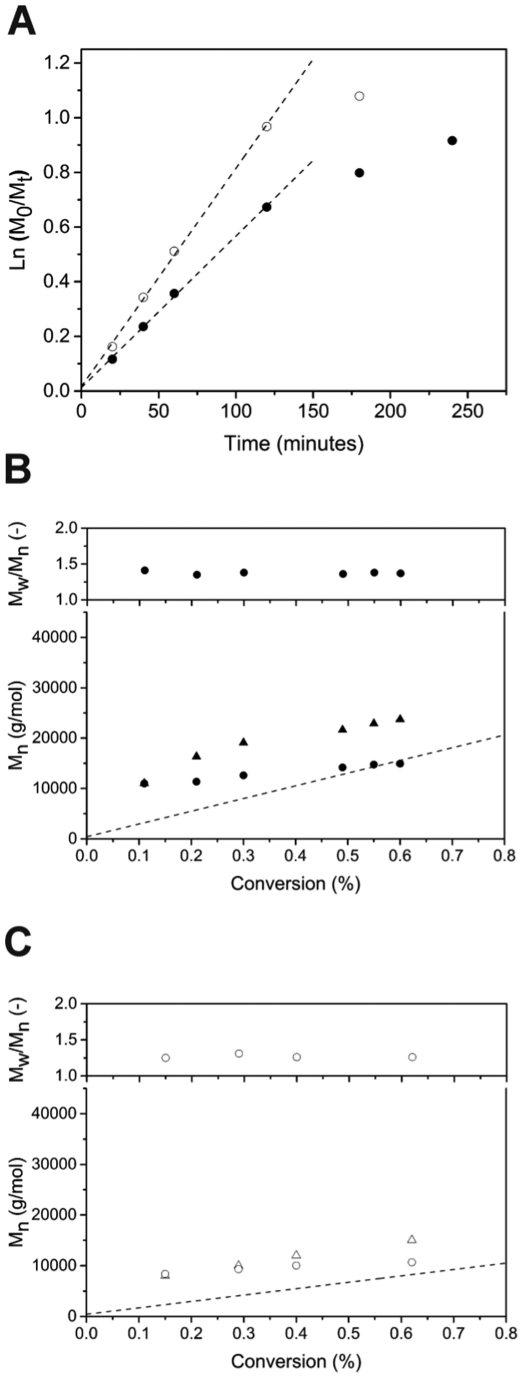

Figure 6. (A) First-order kinetic plot for the **F-CTA-2**-mediated RAFT polymerization of PFMA as determined by ^{19}F NMR spectroscopy. Polymerization conditions: dioxane; 90 °C; $[M]_0$ = 1.8 M; $[M]_0$:[**F-CTA-2**]$_0$ = 100 (●) and 50 (○); [**F-CTA-2**]$_0$:$[I]_0$ = 10. (B) Evolution of experimental M_n and M_w/M_n as a function of monomer conversion for $[M]_0$:[**F-CTA-2**]$_0$ = 100 as determined by SEC (●) and ^{19}F NMR (▲) and (C) $[M]_0$:[**F-CTA-2**]$_0$ = 50 as determined by SEC (○) and ^{19}F NMR (Δ). SEC analysis was performed using THF as solvent, and PS standards were used for conventional calibration. The dashed lines indicate the theoretical M_n (M_n^{TH}) expected for the different conditions.

The resulting C_{tr} and C_{-tr} values for **F-CTA-2** were 4.0 and 390.1 and 4.8 and 370.1 for $[M]_0$:$[CTA]_0$ = 100 and 50, respectively (Table 1). These numbers are close to those obtained for **F-CTA-1** at the same polymerization temperature,

Table 2. ω/α End-Group Ratios Determined via ^{19}F NMR Spectroscopy for the Different PFMA Polymerization Times Using F-CTA-2, $[M]_0$:[F-CTA-2]$_0$ = 100 and 50, and T = 90 °C

[M]:[F-CTA-2]	time (min)	ω/α
100	20	0.97
	40	1.07
	60	0.97
	120	0.88
	180	0.87
	240	0.91
50	20	0.95
	40	0.9
	60	0.92
	120	0.86

which indicates that (i) the introduction of a fluorinated label at the Z-group of **F-CTA-2** does not significantly affect the reactivity of **F-CTA-2** compared to that of **F-CTA-1** and (ii) the polymerization of PFMA with **F-CTA-2** is best described as a hybrid free-radical RAFT polymerization process (as it was the case for **F-CTA-1**, as discussed above).

The difference in ^{19}F NMR chemical shifts of CF_3 groups **A** and **B** in **F-CTA-2** can be used to assess the end-group fidelity of the PPFMA polymers produced with this CTA (Figure 5). The end-group fidelity, expressed as ω/α ratio, was calculated directly using the integrals derived from the **A** (α) and **B** (ω) fluorine peaks incorporated in the polymer. It should be mentioned that due to the presence of initiator-derived side chains, the ω/α values might be slightly overestimated; however, in general, when high $[CTA]_0$:$[I]_0$ ratios are used, the extent of polymer chains lacking α-end-group functionalities can be neglected.[61] The obtained ω/α ratios for the two polymerization conditions for the different polymerization times are reported in Table 2. It was found that for both conditions, the initial ω/α ratios were close to unity and only slightly decreased up to values around 0.86 upon increasing the polymerization time. This suggests that only a minor loss of ω-end groups might occur during the course of the polymerization.

Postpolymerization Modification. After studying the ability of **F-CTA-1** and **F-CTA-2** to mediate the RAFT polymerization of PFMA, the postpolymerization modification of the resulting polymers to generate double chain-end-labeled PHPMA polymers containing a ^{19}F label at the α-terminus and a Rhodamine Red label at the other chain end was assessed (Scheme 2). To this end, the α-fluorinated PPFMA precursor (M_n = 30 200 g/mol by SEC) was first postmodified with 1-amino-2-propanol to give the corresponding α-fluorinated PHPMA derivative. Comparison of the ^{19}F NMR spectra of the PPFMA precursor (Figure 7A) and the corresponding PHPMA derivative (Figure 7B) suggests quantitative aminolysis of the side-chain pentafluorophenyl ester groups. Subsequently, the ω PHPMA end groups were reduced and the resulting thiol moieties reacted with a maleimide-Rhodamine Red dye via Michael addition. While an excess of 1-amino-2-propanol was used in the first reaction step, the thiol−maleimide coupling of the rhodamine dye was found to proceed much more efficient after an additional $NaBH_4$-mediated reduction, which indicates that presumably not all thioester end groups were cleaved via aminolysis by 1-amino-2-propanol. The ^{19}F NMR spectra of the α-fluorinated PPFMA

DOI: 10.1021/acsomega.8b01654
ACS Omega 2018, 3, 9710−9721

Scheme 2. Synthesis of α-Fluorinated, ω-Rhodamine Red-Labeled PHPMA

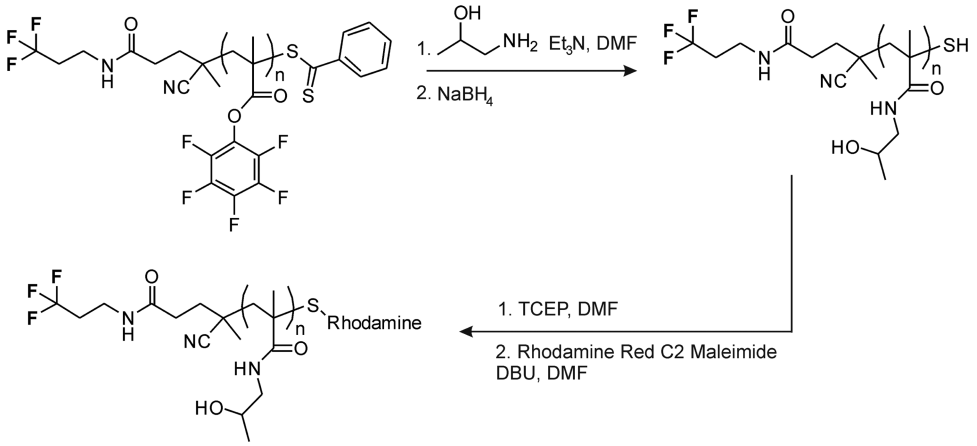

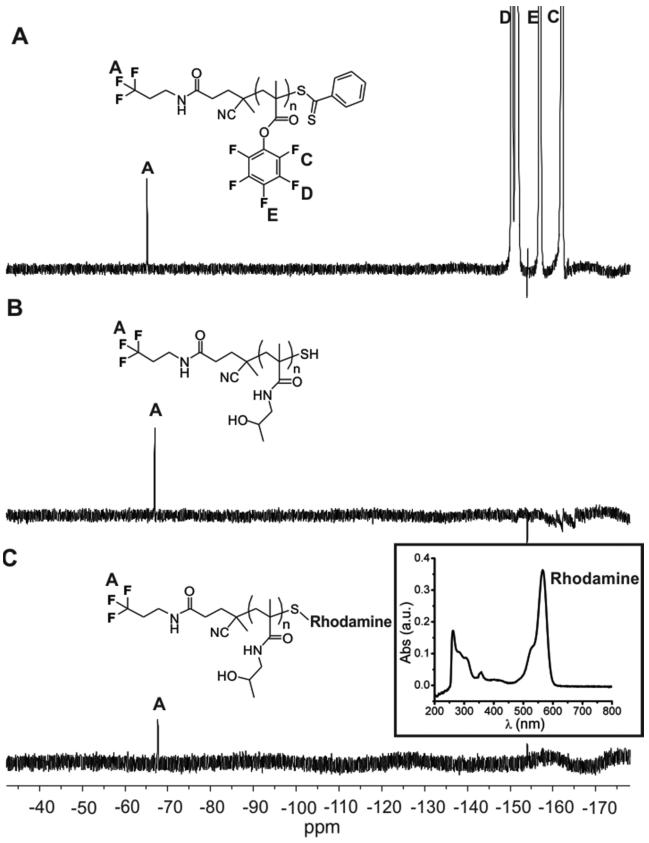

Figure 7. ^{19}F NMR spectra of (A) α-fluorinated PPFMA, (B) α-fluorinated, and (C) α-fluorinated, ω-Rhodamine Red−PHPMA conjugate. The inset in (C) shows the UV−vis spectrum of the α-fluorinated, ω-Rhodamine Red−PHPMA conjugate, which was recorded in dimethyl sulfoxide at a concentration of 0.07 mg/mL.

precursor, the α-fluorinated PHPMA, and the α-fluorinated PHPMA−rhodamine conjugate are shown in Figure 7. The percentage of end-group functionalization with the fluorescent dye was determined by UV spectroscopy measurements using the calibration curve reported in Figure S12 and was estimated to be 80%.

CONCLUSIONS

^{19}F-labeled PHPMA polymers are a potentially interesting platform to generate polymer nanomedicines whose cellular internalization and intracellular trafficking can be monitored using fluorescent label-free techniques, such as NanoSIMS. A first important step toward such polymers is to develop synthetic protocols that allow access to these ^{19}F chain-end-labeled materials. This paper has elaborated a synthetic strategy that is based on the RAFT polymerization of PFMA, mediated by two new RAFT CTAs that contain either 1 (**F-CTA-1**) or 2 (**F-CTA-2**) ^{19}F-labels, followed by postpolymerization modification of the PFMA side-chain functional groups. The polymerization properties of the fluorinated CTAs were investigated in depth and compared to that of 4-cyanopentanoic acid dithiobenzoate (**CTA-1**), which is frequently used for the RAFT polymerization of PFMA. ^{19}F NMR spectroscopy revealed that these two RAFT agents possessed unique chemical shifts that allowed to directly monitor CTA conversion (as well as to determine end-group fidelity). It was found that the introduction of 1 or 2 fluorine labels does not significantly alter the polymerization behavior of the CTAs. For both **CTA-1** and the two fluorinated analogues, the polymerization of PFMA was found to proceed via a hybrid free-radical RAFT mechanism. ^{19}F NMR analysis of polymers produced using **F-CTA-2** revealed end-group fidelities of ∼90%. These ^{19}F-labeled reactive PPFMA polymers are attractive precursors for the synthesis of PHPMA-based polymer nanomedicines. As a first proof of concept, an α-^{19}F-labeled PPFMA was converted via a three-step postpolymerization strategy into an α-^{19}F, ω-Rhodamine Red-labeled PHPMA polymer. Access to such double-labeled polymers is crucial to further the understanding of the cellular internalization and intracellular trafficking of polymer−drug conjugates. While the Rhodamine Red label allows to monitor uptake via flow cytometry or confocal microscopy, the ^{19}F label opens the way to high-resolution mapping of intracellular pathways using NanoSIMS.

EXPERIMENTAL SECTION

Materials. All chemicals were used as received unless described otherwise. 4-Cyanopentanoic acid dithiobenzoate (CTA) (>97%), *N*-(3-dimethylaminopropyl)-*N*′-ethylcarbodiimide hydrochloride (EDC·HCl) (97%), and 2,2′-azobis(2-methylpropionitrile) (98%) (AIBN), which was recrystallized from methanol prior use, tris(2-carboxyethyl)phosphine hydrochloride (TCEP), 1-amino-2-propanol, sodium borohydride ($NaBH_4$), Sephadex G 15, and 1,8-diazabicyclo[5.4.0]undec-7-ene (DBU) were purchased from Sigma-Aldrich. 1,4-Dioxane

DOI: 10.1021/acsomega.8b01654
ACS Omega 2018, 3, 9710−9721

and triethylamine (Et_3N) were purchased from Acros Organics, and 3,3,3-trifluoropropylamine hydrochloride was obtained from Apollo Scientific. Rhodamine Red C2 maleimide was purchased from Life Technologies. Pentafluorophenol was purchased from Matrix Scientific. Dichloromethane (DCM), tetrahydrofuran (THF), hexane, and ethyl acetate were purchased from Reactolab. Sodium methoxide (30% solution in methanol), elemental sulfur, 4-chlorobenzotrifluoride, and 4,4′-azobis(4-cyanovaleric acid), which was crystallized from ethanol, were purchased from J&K Scientific Ltd. Pentafluorophenyl methacrylate (PFMA) was synthesized as reported by Eberhardt et al.[42] 1,4-Dioxane was dried over molecular sieves, and Et_3N was freshly distilled prior use. THF was dried using a Pure Solv solvent purification system prior use.

Methods. *NMR Spectroscopy.* ^1H and ^{19}F NMR spectra were recorded on a Bruker AV-400 instrument at room temperature using $CDCl_3$ as solvent. ^1H NMR chemical shifts are reported relative to the residual proton signal of the solvent.

Size Exclusion Chromatography (SEC). Size exclusion chromatography (SEC) was performed using an Agilent 1260 infinity system equipped with a Varian 390-LC refractive index detector, two PLgel 5 μm Mixed C (Agilent) columns, and a PLgel guard column. THF was used as eluent with a flow rate of 1 mL/min, and the temperature was 40 °C. The samples were analyzed using conventional calibration with polystyrene (PS) standards ranging from 4910 Da to 549 kDa.

UV−vis Spectroscopy. The incorporation of Rhodamine Red C2 maleimide on the polymer was quantified using a Varian Cary 100 Bio spectrometer using quartz cuvettes.

Procedures. *Synthesis of F-CTA-1.* The synthesis of **F-CTA-1** is outlined in Scheme S1A. 4-Cyanopentanoic acid dithiobenzoate (**CTA-1**, 500.0 mg, 1.79 mmol) and (EDC·HCl) (411.6 mg, 2.15 mmol) were dissolved in 8 mL of dry DCM, and the solution was cooled down to 0 °C and stirred under nitrogen. In a second flask, 214.0 mg (1.43 mmol) of 3,3,3-trifluoropropylamine hydrochloride was dissolved in 8 mL of dry DCM and 250 μL (1.43 mmol) of triethylamine was added. After 10 min, the 3,3,3-trifluoropropylamine solution was added dropwise to the first solution and the reaction was stirred at room temperature for 2 h. After that, the solution was washed with 5% $NaHCO_3$ and brine, dried over $MgSO_4$, and finally dried under vacuum. The crude product was purified by flash chromatography using ethyl acetate/hexane 4.5:5.5 to give a dark pink product (73% yield). ^1H, ^{13}C, and ^{19}F NMR spectra of **F-CTA-1** are included in Figures S13−S15. The electrospray ionization (ESI) mass spectrum image is shown in Figure S16. Anal. calcd for $C_{16}H_{17}F_3N_2OS_2$: C, 51.32; N, 7.48; H, 4.58. Found: C, 52.58; N, 7.41; H, 4.93.

Synthesis of F-CTA-2. The synthesis of **F-CTA-2** is outlined in Scheme S1B. Under a dry, nitrogen atmosphere, a flask was charged with 69.4 g of 30% sodium methoxide solution (0.39 mol), followed by 13.3 g of anhydrous methanol and finally rapid addition of 5.4 g (0.17 mol) of elemental sulfur. The mixture was heated in an oil bath at 70 °C with continuous stirring for 30 min. After that, 15.0 g (0.08 mol) of 4-(chloromethyl)benzotrifluoride was added dropwise via an addition funnel over a period of 1 h. The reaction mixture was kept at 70 °C under a nitrogen atmosphere for 10 h. After this time, the reaction was stopped by cooling down to 0 °C using an ice bath. The salt was removed by filtration, and the solvent was removed in vacuum. Then, 50 mL of deionized water was added to the residue and the solution was filtered again. The crude product was washed with diethyl ether (3 × 40 mL) in an extraction funnel. Diethyl ether (20 mL) and 1.0 M HCl (50 mL) were added, and the product was extracted into the ethereal layer. Deionized water (30 mL) and 1.0 M NaOH (60 mL) were added and the product was extracted to the aqueous layer. Potassium ferricyanide(III) (36.3 g, 0.11 mol) was dissolved in 100 mL of deionized water and then added dropwise to the first solution via an addition funnel over a period of 1 h under vigorous stirring. Then, the solution was transferred to an extraction funnel. Anhydrous ethyl acetate (30 mL) was added to wash the product, and the product was extracted to the ethyl acetate layer. This washing process was repeated two more times. The red solution was dried over anhydrous $MgSO_4$ and in vacuum to remove the solvent at room temperature overnight. The resulting 4,4′-di-trifluoromethyl-di(thiobenzoyl) disulfide was dissolved in 50 mL of anhydrous ethyl acetate, and the solution was transferred to a flask. Dry 4,4′-azobis(4-cyanovaleric acid) (2.6 g, 9.19 mmol) was added to the flask, and the reaction solution was heated at 75 °C for 14 h. After that, the ethyl acetate was removed under vacuum and the crude product was purified by column chromatography using ethyl acetate:hexane (1:1.5) as eluent. The solvent mixture was removed in vacuum and the red oily 4-cyanopentanoic acid-4-(trifluoromethyl) dithiobenzoate (75% yield with respect to 4-(chloromethyl)benzotrifluoride) was kept at 4 °C. Next, 2.0 g (5.8 mmol) of 4-cyanopentanoic acid-4-(trifluoromethyl) dithiobenzoate and 1.34 g (6.96 mmol) of EDC·HCl were dissolved in 20 mL of dry DCM. The solution was cooled down to 0 °C and stirred under nitrogen. In a second flask, 0.7 g (4.60 mmol) of 3,3,3-trifluoropropylamine hydrochloride was dissolved in 10 mL of dry DCM and 465 μL (4.60 mmol) of triethylamine was added. After 10 min, the trifluoropropylamine solution was added dropwise to the first solution and the reaction was stirred at room temperature for 2 h. The solution was washed with 5% $NaHCO_3$ solution and brine, dried over anhydrous $MgSO_4$, and dried under vacuum. The crude product was purified by column chromatography using ethyl acetate/hexane 1:1.5 to give 0.5 g (25% yield with respect to 4-cyanopentanoic acid-4-(trifluoromethyl) dithiobenzoate) of the dark pink **F-CTA-2**. We note that these reaction conditions are not optimized. The low yield of this last step compared to the same reaction for the preparation of **F-CTA-1** is most likely due to loss of material during workup and purification. ^1H, ^{13}C, and ^{19}F NMR spectra of **F-CTA-2** are included in Figures S17−S19. The ESI mass spectrum is shown in Figure S20. Anal. calcd for $C_{17}H_{16}F_6N_2OS_2$: C, 46.15; N, 6.33; H, 3.65. Found: C, 46.95; N, 6.31; H, 3.36.

RAFT Polymerization of PFMA. PFMA (1.4 g, 5.56 mmol) was added to a Schlenk tube, followed by 2.08 mL of dry dioxane containing 0.0028, 0.0055, or 0.011 mmol AIBN and 0.028, 0.055, or 0.11 mmol CTA in the case of [M:CTA] = 200, 100, and 50, respectively. The solutions were degassed by four freeze−pump−thaw cycles, and the tubes were filled with argon. The flasks were immersed in an oil bath at 90 °C or 75 °C. At different time intervals, 150 μL aliquots were removed, 50 μL were diluted in 400 μL $CDCl_3$ for ^{19}F NMR analysis, and the remaining part was precipitated in ice-cold hexane three times. The isolated pink product was dried under vacuum overnight and analyzed by SEC.

Synthesis of α-Fluorinated PHPMA. α-Fluorinated PPFMA (100 mg; M_n = 30 200 g/mol by SEC, 0.397 mmol PFMA

DOI: 10.1021/acsomega.8b01654
ACS Omega 2018, 3, 9710−9721

reactive units) was dissolved in 5 mL of dry dimethylformamide (DMF) (^{1}H and ^{19}F NMR spectra of this polymer are included in Supporting Information Figures S21 and S22). Then, 2 equiv (61 μL, 0.794 mmol) 1-amino-2-propanol and 2 equiv (110 μL, 0.794 mmol) Et_3N were added and the reaction was stirred at 50 °C for 20 h. The product was isolated by three precipitations in ice-cold diethyl ether and subsequently dialyzed against water and lyophilized. The ^{1}H NMR spectrum of the resulting α-fluorinated PHPMA is included in Figure S11.

Synthesis of α-Fluorinated PHPMA–Rhodamine Conjugate. Modification of the polymer end groups with Rhodamine Red was performed as previously reported with some modifications.[7] First, 20 mg (0.00129 mmol end groups) of α-fluorinated PHPMA (M_n = 17 200 g/mol, calculated from the M_n of the precursor α-fluorinated PPFMA) was dissolved in 3 mL of an aqueous 0.5 M $NaBH_4$ solution and stirred at room temperature for 2 h. After that, the solution was dialyzed against water for 48 h and the product was lyophilized. In a second step, 10 mg of the product (0.60 μmol end groups) was dissolved in dry DMF, 5 equiv (0.8 mg, 0.0032 mmol) of neutralized TCEP were added, and the solution was stirred overnight under argon. After 20 h, 5 equiv (2.1 mg) of Rhodamine Red C2 maleimide was added together with one drop of DBU. The solution was stirred under argon at room temperature for another 24 h. The solution was dialyzed against water overnight using a SpectraPor (molecular weight cut-off, 3.5 kDa) membrane to remove the DMF and finally lyophilized. The product was purified by passing it through a Sephadex G 15 column. The purification was repeated twice. The percentage of end-group functionalization was estimated using the calibration curve reported in Figure S12, assuming that the extinction coefficient of the polymer-bound Rhodamine Red is the same as that of the corresponding free dye.

■ ASSOCIATED CONTENT

Supporting Information

The Supporting Information is available free of charge on the ACS Publications website at DOI: 10.1021/acsomega.8b01654.

Tabulated results of the PPFMA polymerization experiments mediated by **CTA-1** and **F-CTA-1** and **F-CTA-2**; scheme outlining the synthesis of **F-CTA-1** and **F-CTA-2**; ^{19}F NMR, ^{13}C NMR, ^{1}H NMR, and ESI-MS characterization data for **F-CTA-1** and **F-CTA-2**; curve fitting results for the determination of C_{tr} and C_{-tr}; ^{1}H NMR data of α-fluorinated PHPMA; and Rhodamine Red maleimide calibration curve (PDF)

■ AUTHOR INFORMATION

Corresponding Author

*E-mail: harm-anton.klok@epfl.ch. Tel: +41 21 693 4866.

ORCID

Harm-Anton Klok: 0000-0003-3365-6543

Notes

The authors declare no competing financial interest.

■ ACKNOWLEDGMENTS

This study was financially supported by Swiss National Science Foundation (SNSF). The authors are grateful to Prof. Patrick Theato for his help and advice on the RAFT polymerization on PFMA.

■ REFERENCES

(1) Beija, M.; Charreyre, M. T.; Martinho, J. M. G. Dye-labelled polymer chains at specific sites: Synthesis by living/controlled polymerization. *Prog. Polym. Sci.* **2011**, *36*, 568−602.

(2) Boyer, C.; Bulmus, V.; Davis, T. P.; Ladmiral, V.; Liu, J. Q.; Perrier, S. Bioapplications of RAFT Polymerization. *Chem. Rev.* **2009**, *109*, 5402−5436.

(3) Moad, G.; Rizzardo, E.; Thang, S. H. Living radical polymerization by the RAFT process. *Aust. J. Chem.* **2005**, *58*, 379−410.

(4) Willcock, H.; O'Reilly, R. K. End group removal and modification of RAFT polymers. *Polym. Chem.* **2010**, *1*, 149−157.

(5) Moad, G.; Rizzardo, E.; Thang, S. H. End-functional polymers, thiocarbonylthio group removal/transformation and reversible addition-fragmentation-chain transfer (RAFT) polymerization. *Polym. Int.* **2011**, *60*, 9−25.

(6) Roth, P. J.; Jochum, F. D.; Zentel, R.; Theato, P. Synthesis of Hetero-Telechelic alpha,omega Bio-Functionalized Polymers. *Biomacromolecules* **2010**, *11*, 238−244.

(7) Scales, C. W.; Convertine, A. J.; McCormick, C. L. Fluorescent labeling of RAFT-generated poly(N-isopropylacrylamide) via a facile maleimide-thiol coupling reaction. *Biomacromolecules* **2006**, *7*, 1389−1392.

(8) York, A. W.; Scales, C. W.; Huang, F. Q.; McCormick, C. L. Facile synthetic procedure for omega, primary amine functionalization directly in water for subsequent fluorescent labeling and potential bioconjugation of RAFT-synthesized (Co)polymers. *Biomacromolecules* **2007**, *8*, 2337−2341.

(9) Richardson, S. C. W.; Wallom, K. L.; Ferguson, E. L.; Deacon, S. P. E.; Davies, M. W.; Powell, A. J.; Piper, R. C.; Duncan, R. The use of fluorescence microscopy to define polymer localisation to the late endocytic compartments in cells that are targets for drug delivery. *J. Controlled Release* **2008**, *127*, 1−11.

(10) Maity, A. R.; Stepensky, D. Limited Efficiency of Drug Delivery to Specific Intracellular Organelles Using Subcellularly "Targeted" Drug Delivery Systems. *Mol. Pharmaceutics* **2016**, *13*, 1−7.

(11) Reisch, A.; Klymchenko, A. S. Fluorescent Polymer Nanoparticles Based on Dyes: Seeking Brighter Tools for Bioimaging. *Small* **2016**, *12*, 1968−1992.

(12) Ostrowski, A.; Nordmeyer, D.; Boreham, A.; Holzhausen, C.; Mundhenk, L.; Graf, C.; Meinke, M. C.; Vogt, A.; Hadam, S.; Lademann, J.; Ruhl, E.; Alexiev, U.; Gruber, A. D. Overview about the localization of nanoparticles in tissue and cellular context by different imaging techniques. *Beilstein J. Nanotechnol.* **2015**, *6*, 263−280.

(13) Snipstad, S.; Hak, S.; Baghirov, H.; Sulheim, E.; Morch, Y.; Lelu, S.; Von Haartman, E.; Back, M.; Nilsson, K. P.; Klymchenko, A. S.; De Lange Davies, C.; Aslund, A. K. Labeling nanoparticles: Dye leakage and altered cellular uptake. *Cytometry, Part A* **2016**, *91*, 760−766.

(14) Szeto, H. H.; Schiller, P. W.; Zhao, K.; Luo, G. Fluorescent dyes alter intracellular targeting and function of cell-penetrating tetrapeptides. *FASEB J.* **2005**, *19*, 118−120.

(15) Battistella, C.; Klok, H.-A. Controlling and Monitoring Intracellular Delivery of Anticancer Polymer Nanomedicines. *Macromol. Biosci.* **2017**, *17*, No. 1700022.

(16) Hu, F.; Brucks, S. D.; Lambert, T. H.; Campos, L. M.; Min, W. Stimulated Raman scattering of polymer nanoparticles for multiplexed live-cell imaging. *Chem. Commun.* **2017**, *53*, 6187−6190.

(17) Wei, L.; Hu, F.; Chen, Z.; Shen, Y.; Zhang, L.; Min, W. Live-Cell Bioorthogonal Chemical Imaging: Stimulated Raman Scattering Microscopy of Vibrational Probes. *Acc. Chem. Res.* **2016**, *49*, 1494−1502.

(18) Kubryk, P.; Kolschbach, J. S.; Marozava, S.; Lueders, T.; Meckenstock, R. U.; Niessner, R.; Ivleva, N. P. Exploring the Potential of Stable Isotope (Resonance) Raman Microspectroscopy and

DOI: 10.1021/acsomega.8b01654
ACS Omega 2018, 3, 9710−9721

Surface-Enhanced Raman Scattering for the Analysis of Microorganisms at Single Cell Level. *Anal. Chem.* **2015**, *87*, 6622−6630.
(19) Chen, Z.; Paley, D. W.; Wei, L.; Weisman, A. L.; Friesner, R. A.; Nuckolls, C.; Min, W. Multicolor Live-Cell Chemical Imaging by Isotopically Edited Alkyne Vibrational Palette. *J. Am. Chem. Soc.* **2014**, *136*, 8027−8033.
(20) Proetto, M. T.; Anderton, C. R.; Hu, D.; Szymanski, C. J.; Zhu, Z.; Patterson, J. P.; Kammeyer, J. K.; Nilewski, L. G.; Rush, A. M.; Bell, N. C.; Evans, J. E.; Orr, G.; Howell, S. B.; Gianneschi, N. C. Cellular Delivery of Nanoparticles Revealed with Combined Optical and Isotopic Nanoscopy. *ACS Nano* **2016**, *10*, 4046−4054.
(21) Lee, R. F.; Escrig, S.; Croisier, M.; Clerc-Rosset, S.; Knott, G. W.; Meibom, A.; Davey, C. A.; Johnsson, K.; Dyson, P. J. NanoSIMS analysis of an isotopically labelled organometallic ruthenium(II) drug to probe its distribution and state in vitro. *Chem. Commun.* **2015**, *51*, 16486−16489.
(22) Legin, A. A.; Schintlmeister, A.; Jakupec, M. A.; Galanski, M.; Lichtscheidl, I.; Wagner, M.; Keppler, B. K. NanoSIMS combined with fluorescence microscopy as a tool for subcellular imaging of isotopically labeled platinum-based anticancer drugs. *Chem. Sci.* **2014**, *5*, 3135−3143.
(23) Sheridan, E. J.; Austin, C. J.; Aitken, J. B.; Vogt, S.; Jolliffe, K. A.; Harris, H. H.; Rendina, L. M. Synchrotron X-ray fluorescence studies of a bromine-labelled cyclic RGD peptide interacting with individual tumor cells. *J. Synchrotron Radiat.* **2013**, *20*, 226−233.
(24) Kashiv, Y.; Austin, J. R., II; Lai, B.; Rose, V.; Vogt, S.; El-Muayed, M. Imaging trace element distributions in single organelles and subcellular features. *Sci. Rep.* **2016**, *6*, No. 21437.
(25) Laforce, B.; Carlier, C.; Vekemans, B.; Villanova, J.; Tucoulou, R.; Ceelen, W.; Vincze, L. Assessment of Ovarian Cancer Tumors Treated with Intraperitoneal Cisplatin Therapy by Nanoscopic X-ray Fluorescence Imaging. *Sci. Rep.* **2016**, *6*, No. 29999.
(26) Shah, P.; Westwell, A. D. The role of fluorine in medicinal chemistry. *J. Enzyme Inhib. Med. Chem.* **2007**, *22*, 527−540.
(27) Menaa, F.; Menaa, B.; Sharts, O. Development of carbon-fluorine spectroscopy for pharmaceutical and biomedical applications. *Faraday Discuss.* **2011**, *149*, 269−278.
(28) Menaa, F.; Menaa, B.; Sharts, O. N. Spectro-Fluor Technology for Reliable Detection of Proteins and Biomarkers of Disease: A Pioneered Research Study. *Diagnostics* **2014**, *4*, 140−152.
(29) Rolfe, B. E.; Blakey, I.; Squires, O.; Peng, H.; Boase, N. R.; Alexander, C.; Parsons, P. G.; Boyle, G. M.; Whittaker, A. K.; Thurecht, K. J. Multimodal polymer nanoparticles with combined 19F magnetic resonance and optical detection for tunable, targeted, multimodal imaging in vivo. *J. Am. Chem. Soc.* **2014**, *136*, 2413−2419.
(30) Du, W.; Xu, Z.; Nystrom, A. M.; Zhang, K.; Leonard, J. R.; Wooley, K. L. 19F- and fluorescently labeled micelles as nanoscopic assemblies for chemotherapeutic delivery. *Bioconjugate Chem.* **2008**, *19*, 2492−2498.
(31) Destarac, M.; Bzducha, W.; Taton, D.; Gauthier-Gillaizeau, I.; Zard, S. Z. Xanthates as chain-transfer agents in controlled radical polymerization (MADIX): Structural effect of the O-alkyl group. *Macromol. Rapid Commun.* **2002**, *23*, 1049−1054.
(32) Chapon, P.; Mignaud, C.; Lizarraga, G.; Destarac, M. Automated parallel synthesis of MADIX (Co)Polymers. *Macromol. Rapid Commun.* **2003**, *24*, 87−91.
(33) Adamy, M.; Van Herk, A. M.; Destarac, M.; Monteiro, M. J. Influence of the chemical structure of MADIX agents on the RAFT polymerization of styrene. *Macromolecules* **2003**, *36*, 2293−2301.
(34) Benaglia, M.; Rizzardo, E.; Alberti, A.; Guerra, M. Searching for more effective agents and conditions for the RAFT polymerization of MMA: Influence of dithioester substituents, solvent, and temperature. *Macromolecules* **2005**, *38*, 3129−3140.
(35) Monteiro, M. J.; Adamy, M. M.; Leeuwen, B. J.; Van Herk, A. M.; Destarac, M. A. A "living" radical ab initio emulsion polymerization of styrene using a fluorinated xanthate agent. *Macromolecules* **2005**, *38*, 1538−1541.
(36) Huang, Z. H.; Pan, P. J.; Bao, Y. Z. Solution and Aqueous Miniemulsion Polymerization of Vinyl Chloride Mediated by a Fluorinated Xanthate. *J. Polym. Sci. Part A: Polym. Chem.* **2016**, *54*, 2092−2101.
(37) Huang, Z. H.; Pan, P. J.; Bao, Y. Z. Synthesis of random and block copolymers of vinyl chloride and vinyl acetate by RAFT miniemulsion polymerizations mediated by a fluorinated xanthate. *J. Appl. Polym. Sci.* **2017**, *134*, No. 45074.
(38) Lebreton, P.; Ameduri, B.; Boutevin, B.; Corpart, J. M. Use of original omega-perfluorinated dithioesters for the synthesis of well-controlled polymers by reversible addition-fragmentation chain transfer (RAFT). *Macromol. Chem. Phys.* **2002**, *203*, 522−537.
(39) Bergius, W. N. A.; Hutchings, L. R.; Sarih, N. M.; Thompson, R. L.; Jeschke, M.; Fisher, R. Synthesis and characterisation of end-functionalised poly(N-vinylpyrrolidone) additives by reversible addition-fragmentation transfer polymerisation. *Polym. Chem.* **2013**, *4*, 2815−2827.
(40) Günay, K. A.; Theato, P.; Klok, H.-A. Standing on the shoulders of hermann staudinger: Post-polymerization modification from past to present. *J. Polym. Sci. A Polym. Chem.* **2013**, *51*, 1−28.
(41) Das, A.; Theato, P. Activated ester containing polymers: opportunities and challenges for the design of functional macromolecules. *Chem. Rev.* **2016**, *116*, 1434−1495.
(42) Eberhardt, M.; Mruk, R.; Zentel, R.; Theato, P. Synthesis of pentafluorophenyl(meth)acrylate polymers: New precursor polymers for the synthesis of multifunctional materials. *Eur. Polym. J.* **2005**, *41*, 1569−1575.
(43) Gibson, M. I.; Frohlich, E.; Klok, H.-.A. Postpolymerization Modification of Poly(Pentafluorophenyl methacrylate): Synthesis of a Diverse Water-Soluble Polymer Library. *J. Polym. Sci. A Polym. Chem.* **2009**, *47*, 4332−4345.
(44) Barz, M.; Canal, F.; Koynov, K.; Zentel, R.; Vicent, M. J. Synthesis and in vitro evaluation of defined HPMA folate conjugates: influence of aggregation on folate receptor (FR) mediated cellular uptake. *Biomacromolecules* **2010**, *11*, 2274−2282.
(45) Mohr, N.; Barz, M.; Forst, R.; Zentel, R. A Deeper Insight into the Postpolymerization Modification of Polypenta Fluorophenyl Methacrylates to Poly(N-(2-Hydroxypropyl) Methacrylamide. *Macromol. Rapid Commun.* **2014**, *35*, 1522−1527.
(46) Barz, M.; Luxenhofer, R.; Zentel, R.; Kabanov, A. V. The uptake of N-(2-hydroxypropyl)-methacrylamide based homo, random and block copolymers by human multi-drug resistant breast adenocarcinoma cells. *Biomaterials* **2009**, *30*, 5682−5690.
(47) Nuhn, L.; Hirsch, M.; Krieg, B.; Koynov, K.; Fischer, K.; Schmidt, M.; Helm, M.; Zentel, R. Cationic Nanohydrogel Particles as Potential siRNA Carriers for Cellular Delivery. *ACS Nano* **2012**, *6*, 2198−2214.
(48) Tucker, B. S.; Sumerlin, B. S. Poly(N-(2-hydroxypropyl) methacrylamide)-based nanotherapeutics. *Polym. Chem.* **2014**, *5*, 1566−1572.
(49) Battistella, C.; Klok, H.-A. Reversion of Pgp-mediated drug resistance in ovarian carcinoma cells with PHPMA-Zosuquidar conjugates. *Biomacromolecules* **2017**, *18*, 1855−1865.
(50) Kopecek, J.; Kopeckova, P. HPMA copolymers: Origins, early developments, present, and future. *Adv. Drug Delivery Rev.* **2010**, *62*, 122−149.
(51) Eberhardt, M.; Theato, P. RAFT polymerization of pentafluorophenyl methacrylate: Preparation of reactive linear diblock copolymer. *Macromol. Rapid Commun.* **2005**, *26*, 1488−1493.
(52) Barz, M.; Tarantola, M.; Fischer, K.; Schmidt, M.; Luxenhofer, R.; Janshoff, A.; Theato, P.; Zentel, R. From Defined Reactive Diblock Copolymers to Functional HPMA-Based Self-Assembled Nanoaggregates. *Biomacromolecules* **2008**, *9*, 3114−3118.
(53) Herth, M. M.; Barz, M.; Moderegger, D.; Allmeroth, M.; Jahn, M.; Thews, O.; Zentel, R.; Rosch, F. Radioactive labeling of defined HPMA-based polymeric structures using [18F]FETos for in vivo imaging by positron emission tomography. *Biomacromolecules* **2009**, *10*, 1697−1703.
(54) Barner-Kowollik, C. *Handbook of RAFT polymerization*; Wiley-VCH Verlag GmbH & Co. KGaA: Weinheim, 2008.

DOI: 10.1021/acsomega.8b01654
ACS Omega 2018, 3, 9710−9721

(55) Medeiros, S. F.; Barboza, J. C. S.; Re, M. I.; Giudici, R.; Santos, A. M. Solution Polymerization of N-vinylcaprolactam in 1,4-dioxane. Kinetic Dependence on Temperature, Monomer, and Initiator Concentrations. *J. Appl. Polym. Sci.* **2010**, *118*, 229−240.
(56) Chong, Y. K.; Krstina, J.; Le, T. P. T.; Moad, G.; Postma, A.; Rizzardo, E.; Thang, S. H. Thiocarbonylthio compounds [S═C(Ph)S-R] in free radical polymerization with reversible addition-fragmentation chain transfer (RAFT polymerization). Role of the free-radical leaving group (R). *Macromolecules* **2003**, *36*, 2256−2272.
(57) Pietsch, C.; Fijten, M. W. M.; Lambermont-Thijs, H. M. L.; Hoogenboom, R.; Schubert, U. S. Unexpected Reactivity for the RAFT Copolymerization of Oligo(ethylene glycol) Methacrylates. *J. Polym. Sci., Part A: Polym. Chem.* **2009**, *47*, 2811−2820.
(58) Keddie, D. J.; Moad, G.; Rizzardo, E.; Thang, S. H. RAFT Agent Design and Synthesis. *Macromolecules* **2012**, *45*, 5321−5342.
(59) Han, X. Q.; Fan, J.; He, J. P.; Xu, J. T.; Fan, D. Q.; Yang, Y. L. Direct observation of the RAFT polymerization process by chromatography. *Macromolecules* **2007**, *40*, 5618−5624.
(60) Chiefari, J.; Mayadunne, R. T. A.; Moad, C. L.; Moad, G.; Rizzardo, E.; Postma, A.; Skidmore, M. A.; Thang, S. H. Thiocarbonylthio compounds (S═C(Z)S-R) in free radical polymerization with reversible addition-fragmentation chain transfer (RAFT polymerization). Effect of the activating group Z. *Macromolecules* **2003**, *36*, 2273−2283.
(61) Päch, M.; Zehm, D.; Lange, M.; Dambowsky, I.; Weiss, J.; Laschewsky, A. Universal Polymer Analysis by ^{1}H NMR Using Complementary Trimethylsilyl End Groups. *J. Am. Chem. Soc.* **2010**, *132*, 8757−8765.

DOI: 10.1021/acsomega.8b01654
ACS Omega 2018, 3, 9710−9721